Int. J. Electrochem. Sci., 12 **(2017)** 9478 – 9487, doi: 10.20964/2017.10.19

International Journal of
ELECTROCHEMICAL
SCIENCE
www.electrochemsci.org

Fabrication of an Electrochemical Sensor for Helicobacter pylori in Excrement Based on a Gold Electrode

Puji Peng[1,*], *Feng Xu*[1], *Yuying Xu*[2] *and Shuang Sun*[1]

[1] Zhengzhou University; Zhengzhou, Henan, 450052, China
[2] Henan University of Chinese Medicine, Zhengzhou, Henan 450000, China
[*]E-mail: pengpuji852@163.com

Received: 16 June 2017 / *Accepted:* 29 July 2017 / *Published:* 12 September 2017

This study presented the determination of *Helicobacter pylori* using a gold electrode (AuE)-based electrochemical biosensor in which the electroactive label was β-cyclodextrin (β-CD). The covalent immobilization of a thiol-decorated single-stranded DNA probe on the AuE surface occurred through the formation of a Au–S bond. The DNA hybridization was monitored via the differential pulse voltammetry (DPV) method, where the electrochemical signals for reduction of the β-CD bound to the double-stranded DNA (dsDNA) were measured. The electrochemical signal was linearly related to the target DNA concentration (0.3 nM–0.24 μM) when measured under optimal conditions, and the limit of detection (LOD) was determined to be as low as 0.15 nM, suggesting that measurements with our developed biosensor were highly repeatable and reproducible. In addition, our proposed biosensor was successfully applied to the determination of *Helicobacter pylori* in excrement.

Keywords: Electrochemical biosensor; β-cyclodextrin; *Helicobacter pylori*; Excrement; Thiol modification

1. INTRODUCTION

Helicobacter pylori, abbreviated as *H. pylori*, is a common bacterium that colonizes the stomach, leading to gastritis, gastric ulcers, and possibly even stomach cancer [1, 2]. Urease produced by *H. pylori* can hydrolyse the urea that is naturally present in the stomach into ammonia, causing neutralization of the gastric acid. Hence, the lifespan of the bacteria in the gastric juice is prolonged, resulting in colonization of the gastric mucus. Using the Urea Breath Test (UBT) or the Rapid Urease Test (RUT) [3, 4], those with high urease activity are usually diagnosed with *H. pylori* infection. Despite the present consensus that RUT is the most rapid determination strategy for *H. pylori*, this

strategy still has several disadvantages, such as inaccuracy caused by inadequate stomach acidity or a low concentration of *H. pylori* and the invasive nature of the required endoscopy.

Hence, it is clinically significant to propose a selective and sensitive *H. pylori* DNA sequence determination to monitor and manage the diseases related to *H. pylori* infection. In the last decade, several fabrication methods of biosensors have been reported for the detection of *H. pylori*, such as immune-based biosensors that include sandwiched and enzymatically amplified piezoelectric biosensors [5] as well as the electrokinetically driven microfluidic immunoassay [6, 7], DNA-based biosensors [8, 9], and electrochemical methods [10]. In these determination techniques, DNA hybridization has been considered an excellent method for *H. pylori* determination and identification [11].

Electrochemical biosensors possess several advantages, such as small sample amount, portability, cost-effectiveness, simplicity and desirable sensitivity. [12]. Most electrochemical DNA biosensors are prepared using DNA hybridization [13], and a DNA sequence could be determined using hybridization-involved sequencing [14]. An electrochemical biosensor for DNA determination contains a DNA-immobilized working electrode, and the target DNA interacts with the immobilized probe differently than a non-specific sequence [15]. DNA hybridization techniques primarily include direct and indirect methods, and an electrochemical signal could be obtained from purine base oxidation in the case of the latter technique. However, the indirect technique involves the use of electroactive labels and monitoring of their interaction with DNA strands. In electrochemical-based DNA sensing techniques, the electroactive labels used include methylene blue, haematoxylin, $[Ru(NH_3)_6]^{3+/2+}$[16], and $[Fe(CN)[Co(phen)_3]^{3+/2}$ ferrocene [17].

This study described the fabrication of a novel electrochemical biosensor in which β-CD interacted with a gene of *H. pylori* and the application of the sensor to the determination of *H. pylori* through the hybridization of DNA with the self-assembled monolayer (SAM) strategy.

2. EXPERIMENTS

2.1. Chemicals

All test reagents were used without additional purification. 6-Mercapto-1-hexanol (MCH) was purchased from Aldrich. All other chemicals were commercially available from Aladdin. Doubly distilled water was used for the preparation of all test solutions. Oligonucleotides obtained from Eurofins MWG Operon in the form of lyophilized powders exhibited the sequences below: Thiolated DNA probe (H. pylori): 5′-HS $(CH_2)_6$ AGA CAT GCA AAA AGG TAT-3′. Mismatched DNA (H. pylori): 5′-AGA CAT GCT AAA AGG TAT-3′. Complementary target DNA (H. pylori): 5′-AGA CAT GCA AAA AGG TAT-3′. Non-complementary DNA: 5′-GAA TAT GAT TTA CAG TTT ATT TT-3′. Stock solutions of the oligonucleotides (100.0 μM) were prepared in Tris–HCl buffer (10 mM, pH 8.0) + 1.0 mM EDTA followed by freezing at −20 °C. The β-CD powder was dissolved in methanol and then added to 0.1 M PBS (pH 7.0) for the preparation of the β-CD stock solution (1.0 mM).

2.2. Instrumentations

An electrochemical analyser (CHI832B, CHI Instrument) controlled by a computer was used for the electrochemical assays with a traditional triple-electrode configuration. Under this configuration, the working, reference, and counter electrodes were decorated with AuE, saturated calomel electrode, and platinum wire, respectively.

2.3. Preparation of DNA sensor

AuE surface was polished on a smooth polishing fabric using alumina–water slurry (1.0 μm and 0.0 The AuE surface was polished on a smooth polishing fabric using an alumina–water slurry (1.0 μm and 0.05 μm) followed by rinsing with doubly distilled water and drying in a nitrogen stream. The probe was self-assembled by depositing a 2.5 μL droplet of immobilization buffer solution + *H. pylori* probe (ssDNA) (9.0 μM) on the surface of the AuE followed by incubation of the as-prepared electrode for 60 min at ambient temperature in a high-humidity container to obtain the *H. pylori* self-assembled electrode (ssDNA/AuE). The as-prepared electrode was then washed with the washing solution, incubated in an MCH solution (1.0 mM) for 5 min, and successively rinsed with an ethanol:water mixture (80:20, v/v) and distilled water. The probe was hybridized with the specimen DNA by immersing the as-prepared ssDNA/AuE in a pH 7.0 hybridization buffer solution (HBS) that contained the target oligonucleotide (at the desired concentration for mismatched, complementary or non-complementary strands) for 2 h at ambient temperature, thereby generating the dsDNA/AuE.

The as-prepared electrode was immersed in a 0.1 M phosphate buffer solution (PBS) (pH 7.0) + 0.09 mM β-CD under gentle stirring at 100 rpm for 60 min to accumulate β-CD on the as-prepared dsDNA/AuE, where no potential was applied. This was followed by rinsing the electrode with the washing solution for 10 s. To accumulate β-CD on the original AuE, we carried out a similar procedure.

2.4. Measurements

DPV was used for the electrochemical investigation in pH 7.0 PBS (0.1 M), and the step potential, modulation, and amplitude were 50 mV, 0.05 s, and 25 mV, respectively. The decorated electrode was characterized via electrochemical impedance spectroscopy (EIS) and cyclic voltammetry (CV) measurements in a $K_3[Fe(CN)_6]$ solution. The EIS measurement was carried out in 5.0 mM $K_3[Fe(CN)_6]/K_4[Fe(CN)_6]$ + 1.0 M KCl (100 kHz–0.01 Hz), and the potential amplitudes were 0.27 V and 5 mV, respectively. The CV measurement was carried out in $K_3[Fe(CN)_6]$ (1.0 mM) in PBS (sweep rate, 20 mV/s; potential range, -0.025 to 0.33 V). In addition, the selectivity of our proposed biosensor was evaluated by incubating it in hybridization solutions of the non-complementary and mismatched sequences under the same hybridization conditions, after which DPV voltammograms were obtained.

3. RESULTS AND DISCUSSION

Droplet self-assembly and solution self-assembly techniques were used to immobilize the ssDNA. The former strategy was performed by introducing a 2.5 μL droplet of *H. pylori* probe solution on the original AuE. The other strategy was conducted by immersing the original AuE in immobilization buffer containing the probe (9.0 μM) for 105 min. This was followed by soaking the two separately decorated electrodes in MCH and β-CD solutions successively. The self-assembled AuE probe was then successively immersed in a solution of the target DNA and a β-CD solution since the accumulation of β-CD was observed on the dsDNA-decorated electrode. The accumulated β-CD on the ssDNA/AuE surface was characterized by DPV before and after hybridization with the complementary DNA for the two aforementioned self-assembly strategies, as shown in Fig. 1A.

The β-CD accumulated on the ssDNA-decorated AuE electrode that was prepared using the droplet self-assembly strategy exhibited a larger current response than the other strategy. In addition, compared with the solution self-assembly strategy, the droplet self-assembly strategy contributed to a higher current response after hybridization, indicating that the droplet self-assembly strategy provided more of the desired probe molecules. The accumulated ssDNA/AuE current response was enhanced by increasing the probe immobilization time up to approximately 105 min, after which the response slightly decreased. This may be caused by complete coverage of the gold electrode surface with the DNA probe after 105 min. Therefore, a time of 105 min was chosen for probe immobilization in subsequent experiments [18].

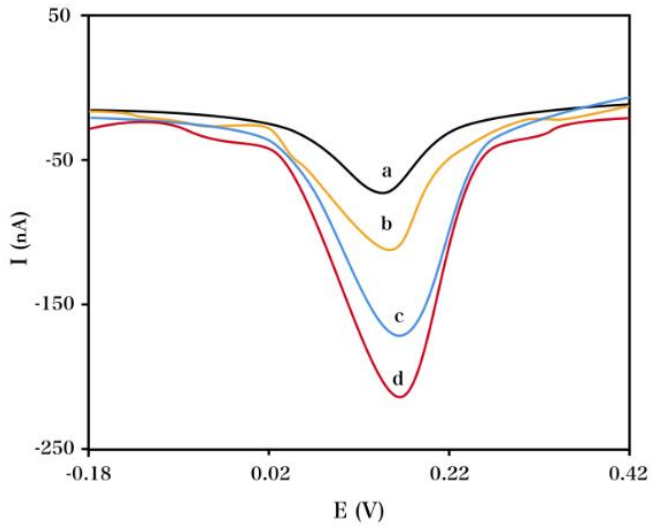

Figure 1. (A) DPVs of the accumulated β-CD on the surface of ssDNA/AuE before (voltammograms a and b) and after hybridization with the complementary DNA (voltammograms c and d) using the electrodes fabricated by the droplet self-assembly technique (voltammograms b and d) and the solution self-assembly technique (voltammograms a and c).

The DNA was hybridized using three techniques, and a comparison of the corresponding results is presented. With respect to the droplet self-assembly strategy, a 2.5 μL droplet of the

complementary solution was deposited on the as-prepared ssDNA-decorated AuE for hybridization followed by incubation in a container (high-humidity) for 120 min at ambient temperature to prevent evaporation. After completely rinsing the decorated electrode with the washing solution and stirring at 100 rpm, we performed the accumulation of β-CD on the surface of the decorated electrode. The current response of the accumulated ssDNA increased and then slightly decreased upon increasing the probe concentration. This is in agreement with the findings of Nasirizadeh and co-workers [13] in which massive accumulation of the probe on the electrode resulted in lower availability of the ssDNA to DNA. The ssDNA accumulated on the surface of the as-prepared electrode was characterized via the DPV profile (Fig. 2). A preheated solution hybridization strategy was conducted by soaking the as-prepared ssDNA-decorated AuE in the hybridization solution at 85 °C under mild stirring for 3 min. This was followed by gradually cooling the above solution to ambient temperature, rinsing the as-prepared electrode with the washing solution, and accumulating β-CD on the electrode. The accumulated β-CD from the preheated solution hybridization strategy was characterized via DPV, as shown in Fig. 2. The decorated electrode was immersed in the β-CD solution after hybridization. The decorated electrode prepared using the solution strategy exhibited the highest current response. It can be concluded that in the solution protocol, the target DNA has a better chance of attaining the best orientation for hybridization.

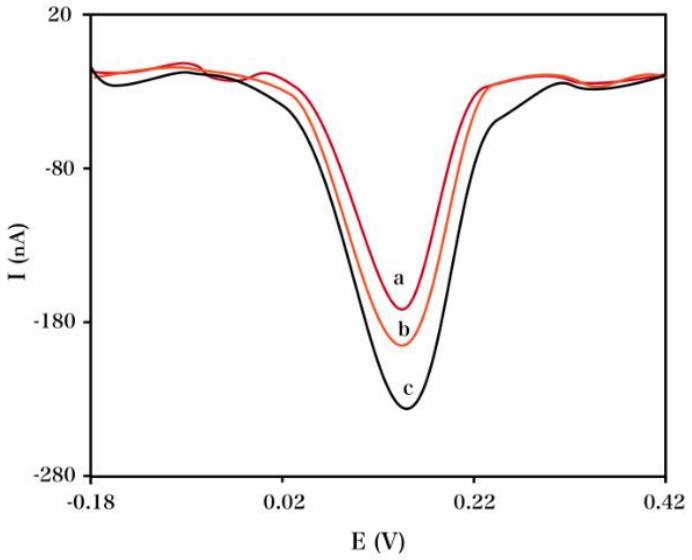

Figure 2. DPVs of the accumulated β-CD on the surface of the dsDNA/SAM prepared using varying hybridization techniques, including (a) drop, (b) preheated solution and (c) solution hybridization.

DPV measurements were performed to investigate the optimal concentration of β-CD (an electroactive label) on the decorated electrode in the presence of dsDNA. Therefore, the hybridization step was followed by immersing the decorated AuE in a solution of β-CD (varying concentrations) for 1.5 h. As displayed in Fig. 3A, the accumulated β-CD was characterized by DPV. As the concentration of β-CD increased, an increase in the signal of accumulated OB was observed. The cathodic current

was highest for a β-CD concentration of 0.9 mM and subsequently reached a plateau. Thus, this value was selected as the optimal β-CD concentration. Furthermore, we also studied the effect of the β-CD accumulation time and determined an optimal time of 90 min for β-CD accumulation on the dsDNA/SAM surface.

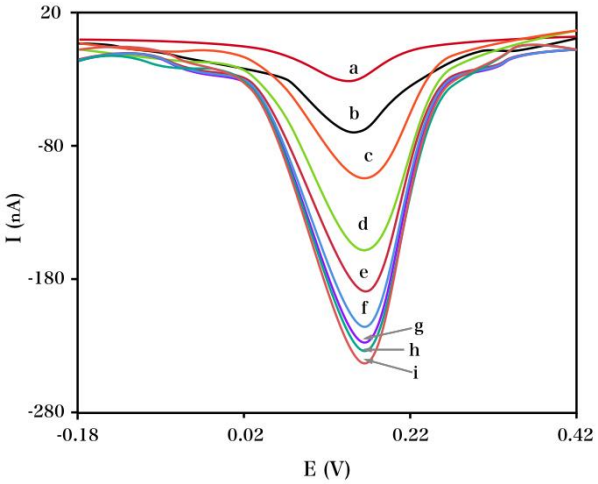

Figure 3. (A) DPVs of the accumulated β-CD on the surface of the dsDNA/SAM prepared with varying concentrations of β-CD. (a) to (i) represent β-CD concentrations from 0.015 to 0.135 mM.

To assess the selectivity of the DNA hybridization on the AuE in the presence of the probe DNA, hybridization with its complete complementary sequence, mismatched sequence, and non-complementary sequence was performed. Characterization of the accumulated β-CD on the MCH/AuE (curve a) and the ssDNA-decorated AuE before (curve b) and after hybridization with non-complementary (curve c), mismatched (curve d) and complementary (curve e) oligonucleotide solutions (2.0 μM) was performed by DPV, as shown in Fig. 4.

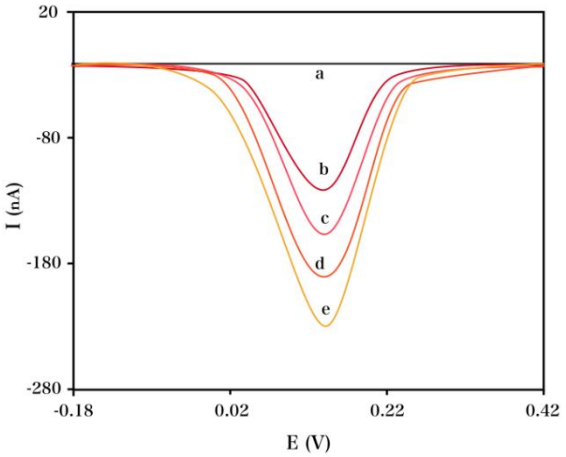

Figure 4. DPVs of the accumulated β-CD on the (a) MCH-decorated AuE and ssDNA-decorated AuE before (b) and after hybridization with oligonucleotide solutions (2 μM) of the (c) non-complementary, (d) mismatched, and (e) complementary sequences in phosphate buffer solution (0.1 M, pH 7.0).

It can be seen that OB exhibited a remarkable peak current increase during hybridization with its complementary sequence compared to the DPV response of β-CD with ssDNA/AuE in the presence of the probe DNA, as displayed in Fig. 4. Compared to hybridization with the non-complementary sequence, that with the mismatched DNA resulted in a higher current peak, suggesting that the decorated electrode has the desired selectivity in the hybridization of DNA.

The decorated electrode after each modification procedure was characterized via CV in a $K_3[Fe(CN)_6]$ solution (1.0 mM), as shown in Fig. 5A. The voltammogram current was high for the original AuE, and an obvious decrease was observed after ssDNA was immobilized on the AuE. This was because the access of $[Fe(CN)_6]^{3-/4-}$ anions to the surface of the AuE was blocked, as shown in curve (b). There was a clear difference in the current for each modification step, which confirmed the successful immobilization and hybridization of each DNA probe. However, the voltammogram current increased after the ssDNA/AuE was treated with MCH due to the incorrect removal of the orientated ssDNA. An obvious decrease in the current was observed after the target DNA was hybridized with the ssDNA on the AuE, while a higher current was obtained in the case of hybridization with the mismatched target DNA since its hybridization with the ssDNA present on the AuE was incomplete.

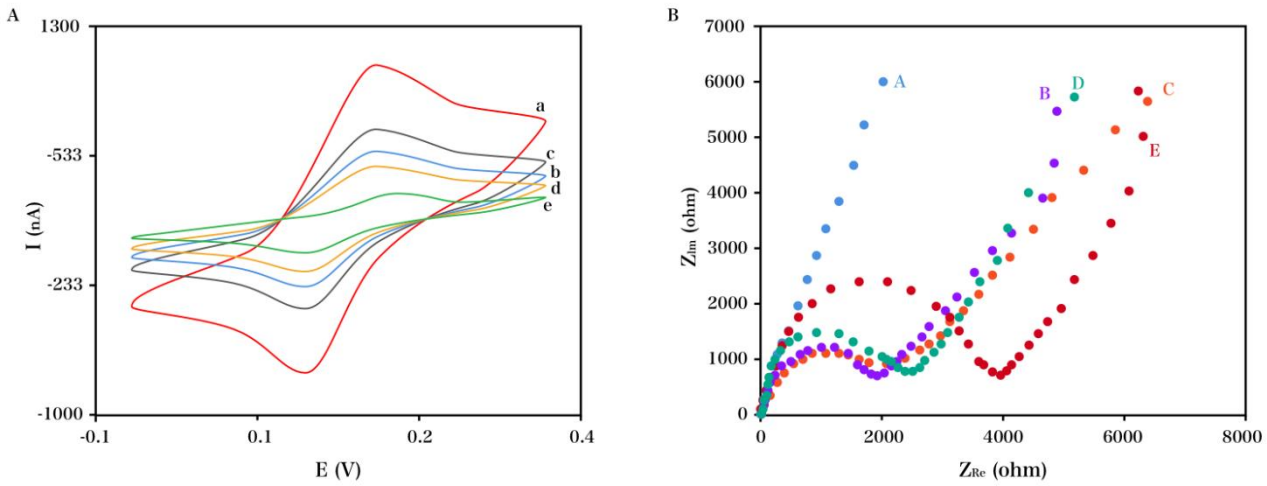

Figure 5. (A) CVs of the decorated electrode in a $K_3[Fe(CN)_6]$ solution (1.0 mM) after each electrode modification step: (a) original AuE, (b) ssDNA-decorated AuE, (c) MCH/ssDNA-decorated AuE, (d) mismatched target DNA, and (e) target DNA. (B) Nyquist plots of the various electrodes in 5.0 mM $K_3[Fe(CN)_6]/K_4[Fe(CN)_6]$ + 1.0 M KCl: (a) original AuE, (b) ssDNA-decorated AuE, (c) MCH/ssDNA-decorated AuE, (d) mismatched target DNA, and (e) target DNA.

The various electrodes were characterized in 5.0 mM $K_3[Fe(CN)_6]/K_4[Fe(CN)_6]$ that also contained 1.0 M KCl using Nyquist plots, as shown in Fig. 5B. The characterization of the original AuE is presented in curve (a), where a rather low resistance was observed. An increase in the charge transfer resistance (R_{ct}) of the electrode was observed after the ssDNA was immobilized on the AuE since the access of the $[Fe(CN)_6]^{3-/4-}$ ions to the surface of the AuE was blocked, as displayed in curve (b). However, a decrease in R_{ct} was observed after the ssDNA/AuE was treated with MCH, as shown

in curve (c). The target hybridized/probe-modified AuE showed a significantly higher charge transfer resistance, but the mismatched target had a significantly lower Rct, which could be because of incomplete hybridization of the mismatched DNA compared to the complementary target DNA. The observations from the abovementioned CV and EIS studies are in agreement and confirm the formation of the proposed biosensor through the electrode modification steps and the good selectivity of the biosensor [19].

The DPV hybridization responses obtained for increasing concentrations of the complementary sequence (0.3 nM–0.24 μM) are shown in Fig. 6A. The inset reveals that as the concentration of the complementary target DNA increased, the peak currents of the intercalated β-CD increased, thereby exhibiting a linear relationship (Fig. 6B). Based on the equation $Cm = 3s_{bl}/m$, an LOD as low as 0.15 Nm was obtained. The analytical features of our developed biosensor are compared those of previous studies in Table 1.

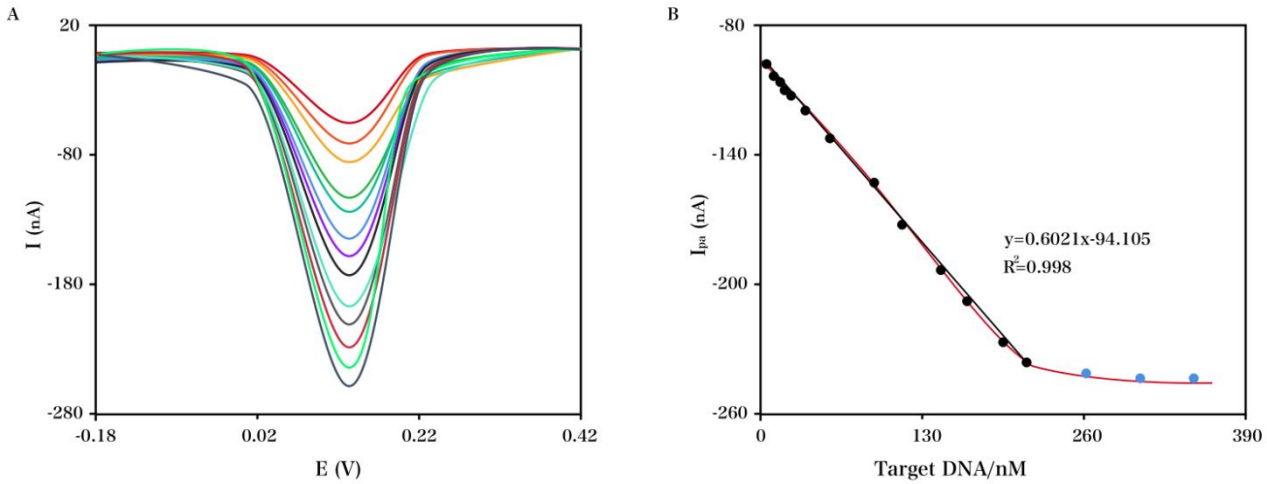

Figure 6. (A) DPVs of the accumulated β-CD on the hybridized ssDNA-decorated AuE with varying concentrations of the complementary (target) DNA in PBS (0.1 M, pH 7.0). (B) Inset: plot of the variation in the accumulated current response for the dsDNA-decorated AuE and ssDNA/SAM *vs.* the concentration of target DNA during hybridization.

Table 1. Comparison of the primary features of the electrochemical sensors applied to *H. pylori* determination.

Method	Linear range (nM)	Detection limit (nM)	Reference
Hematoxylin	12-350	3.8	[13]
Anthraquinone	20-12000	14	[20]
$Co(phen)_3]^{3+}$	0.001-100	0.0002	[21]
Methylene blue	5-100	4.35	[22]
β-CD	0.3-240	0.15	This work

Furthermore, the relative standard deviation (RSD) for all experiments with varying concentrations of the target DNA were as low as 3.2–4.1%, confirming the desirable repeatability of

our developed biosensor. In addition, biosensor fabrication was performed five times, followed by measurements under similar concentrations and circumstances, and the reproducibility of our developed biosensor was assessed based on the comparison of corresponding results. A low RSD (4.0%) was obtained after the biosensor fabrication was performed five times, suggesting that our developed biosensor was highly reproducible.

A recovery test was performed to assess the accuracy of our DNA sensor developed for excrement detection. All excrement specimens were collected in 0.22 μm ethanol, double-filtered, and then stored at 4 °C if not used immediately. The results suggested a desirable consistency between the electrochemical detection and the ELISA method. The accuracy of our developed biosensor was assessed by mixing varying concentrations of *H. pylori* with the specimens, as well as by recovery tests. The results in Table 2 suggest the excellent accuracy of our developed biosensor and its potential application as a parallel technique for real samples.

Table 2. *H. pylori* detection in real beef specimens based on our developed DNA sensor using ELISA strategy.

Added (nM)	Immunosensor			ELISA		
	Found (nM)	Recovery (%)	RSD (%)	Found (nM)	Recovery (%)	RSD (%)
5	4.96	99.2	1.7	4.92	98.4	2.9
10	9.81	98.1	2.6	10.10	101.0	3.6
20	20.19	100.95	3.1	20.15	100.75	1.5

4. CONCLUSIONS

This work studied the interactions of a β-CD (electroactive DNA label)-based sensor for *H. pylori*. The affinity and specificity of the DNA biosensor towards *H. pylori* (corresponding to oligonucleotides from non-complementary DNA) was determined through the investigation of β-CD interactions with varying dsDNA and ssDNA sensors. The results indicated that the β-CD-based DNA biosensor could detect a single base mismatch in the target DNA. In addition, the optimal hybridization strategy and probe self-assembly technique were solution hybridization and drop self-assembly, respectively. The electrical signal was found to be linearly related to the target DNA concentration (0.3 nM–0.24 μM) under optimal conditions, with an LOD of 0.15 nM.

References

1. E. Sweeney, J. Henderson, J. Goers, C. Wreden, K.G. Hicks, J.K. Foster, R. Parthasarathy, S. Remington and K. Guillemin, *Structure*, 20 (2012) 1177.
2. J.P. Celli, B.S. Turner, N.H. Afdhal, S. Keates, I. Ghiran, C.P. Kelly, R.H. Ewoldt, G.H. McKinley, P. So and S. Erramilli, *Proceedings of the National Academy of Sciences*, 106 (2009) 14321.
3. A.I. Lopes, F.F. Vale and M. Oleastro, *World journal of gastroenterology*, 20 (2014) 9299.
4. C.H. Viiala, H.M. Windsor, G.M. Forbes, S.O. Chairman, B.J. Marshall and L.C. Mollison, *Journal*

of gastroenterology and hepatology, 17 (2002) 127.
5. X. Su and S.F. Li, *Anal. Chim. Acta.*, 429 (2001) 27.
6. Q. Chen, J. Zhao, H. Zhang and X. Wang, *Anal. Chim. Acta.*, 572 (2006) 77.
7. M.A. Seia, S.V. Pereira, C.A. Fontán, I.E. De Vito, G.A. Messina and J. Raba, *Sensors and Actuators B: Chemical*, 168 (2012) 297.
8. M. Del Pozo, C. Alonso, F. Pariente and E. Lorenzo, *Anal. Chem.*, 77 (2005) 2550.
9. T. García, E. Casero, M. Revenga-Parra, J. Martín-Benito, F. Pariente, L. Vázquez and E. Lorenzo, *Biosensors and Bioelectronics*, 24 (2008) 184.
10. C. Sun, L. Zhang, J. Jiang, G. Shen and R. Yu, *Biosensors and Bioelectronics*, 25 (2010) 2483.
11. H.-F. Cui, T.-B. Xu, Y.-L. Sun, A.-W. Zhou, Y.-H. Cui, W. Liu and J.H. Luong, *Anal. Chem.*, 87 (2015) 1358.
12. Y. Hu, X. Xu, Q. Liu, L. Wang, Z. Lin and G. Chen, *Anal. Chem.*, 86 (2014) 8785.
13. N. Nasirizadeh, H.R. Zare, M.H. Pournaghi-Azar and M.S. Hejazi, *Biosensors and Bioelectronics*, 26 (2011) 2638.
14. H. Jin, M. Wei and J. Wang, *Chemistry Central Journal*, 7 (2013) 65.
15. J.B. Raoof, R. Ojani, S.M. Golabi, E. Hamidi-Asl and M.S. Hejazi, *Sensors and Actuators B: Chemical*, 157 (2011) 195.
16. S.W. Dutse, N.A. Yusof, H. Ahmad, M.Z. Hussein and Z. Zainal, *Int J Electrochem Sci*, 7 (2012) 8105.
17. X. Luo, T.M.-H. Lee and I.-M. Hsing, *Anal. Chem.*, 80 (2008) 7341.
18. P.A. Rasheed and N. Sandhyarani, *Sensors and Actuators B: Chemical*, 204 (2014) 777.
19. L. Wu, E. Xiong, X. Zhang, X. Zhang and J. Chen, *Nano Today*, 9 (2014) 197.
20. S. Hajihosseini, N. Nasirizadeh, M.S. Hejazi and P. Yaghmaei, *Materials Science and Engineering: C*, 61 (2016) 506.
21. Z. Shakoori, S. Salimian, S. Kharrazi, M. Adabi and R. Saber, *Anal Bioanal Chem*, 407 (2015) 455.
22. D.S. Campos-Ferreira, G.A. Nascimento, E.V. Souza, M.A. Souto-Maior, M.S. Arruda, D.M. Zanforlin, M.H. Ekert, D. Bruneska and J.L. Lima-Filho, *Anal. Chim. Acta.*, 804 (2013) 258.